Proton conductivity of mesoporous aluminum organophosphonate enhanced by the affinity of integral organic linker to water molecule

Takahiro Ami,[a] Kouki Oka,*[a,b,c] Hitoshi Kasai[a] and Tatsuo Kimura*[d]

[a] Institute of Multidisciplinary Research for Advanced Materials, Tohoku University, 2-1-1 Katahira, Aoba-ku, Sendai, Miyagi 980-8577, Japan.
[b] Carbon Recycling Energy Research Center Ibaraki University, 4-12-1 Nakanarusawa, Hitachi, Ibaraki 316-8511, Japan.
[c] Deuterium Science Research Unit, Center for the Promotion of Interdisciplinary Education and Research Kyoto University, Yoshida, Sakyo-ku, Kyoto 606-8501, Japan.
*E-mail: oka@tohoku.ac.jp
[d] National Institute of Advanced Industrial Science and Technology (AIST), Sakurazaka, Moriyama-ku, Nagoya 463-8560, Japan.
*E-mail: t-kimura@aist.go.jp

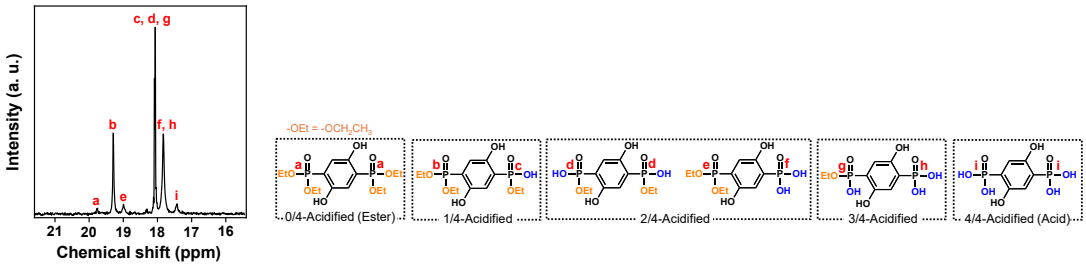

Fig. S1 ^{31}P NMR spectrum (chloroform-d_1) of the partially acidified $(H_5C_2O)_2$OP-HQ-PO$(OC_2H_5)_2$. The -ethoxy (-OC_2H_5) group was expressed as -OEt in the figure. All the peaks were assigned to P atoms in the partially acidified compounds, indicating that all the parent $(H_5C_2O)_2$OP-HQ-PO$(OC_2H_5)_2$ was acidified but not to acidified completely.

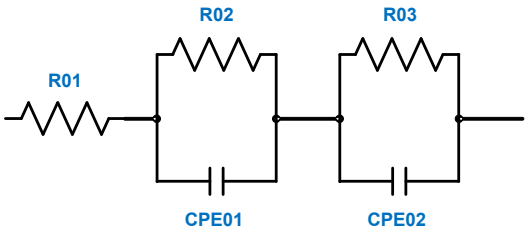

Fig. S2 Equivalent circuit for fitting analysis to calculate proton conductivity**.**

*The equivalent circuit considered the resistance of cables and bulk and grain boundary resistances in the impedance measurement.
*CPE was calculated by following the formula CPE = $\{T(i2\pi f)^{\alpha}\}^{-1}$ ($0 \leq \alpha \leq 1$, $i^2 = -1$), where T and f were a CPE constant and frequency, respectively.

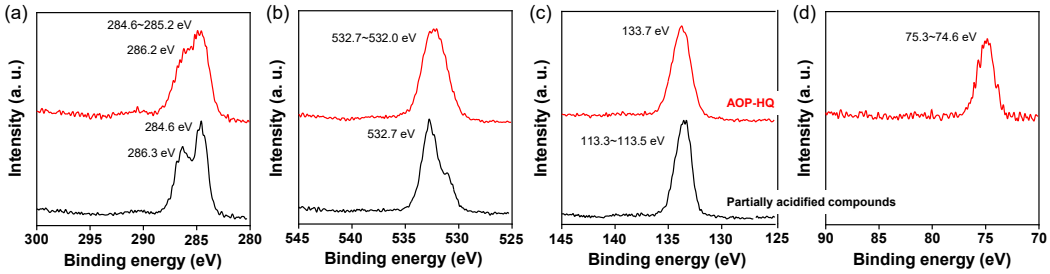

Fig. S3 (a) C 1s, (b) O 1s, (c) P 2p and (d) Al 2p XPS spectra of AOP-HQ and the partially acidified compounds arising from $(H_5C_2O)_2$OP-HQ-PO$(OC_2H_5)_2$.

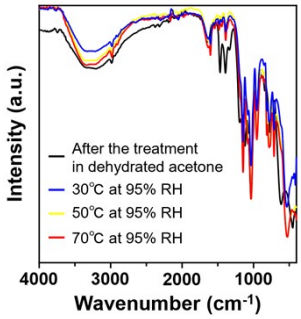

Fig. S4 Temperature-dependent FT-IR spectra of AOP-HQ under humid conditions (95% RH) at 30 °C, 50 °C and 70 °Cwith the original spectrum before the measurement.

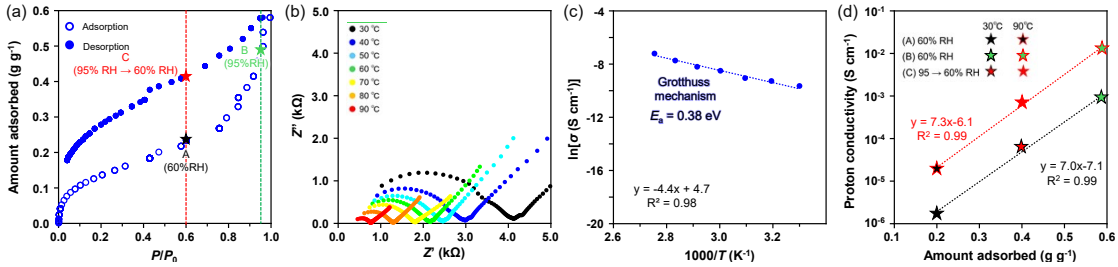

Fig. S5 (a) H_2O adsorption-desorption isotherm of AOP- HQ, (b) impedance spectra of the disk-shaped pellet at temperatures ranging from 30 °C to 90 °C, (c) the Arrhenius plot of the proton conductivity and (d) correlation between proton conductivity and adsorbed amount of H_2O.

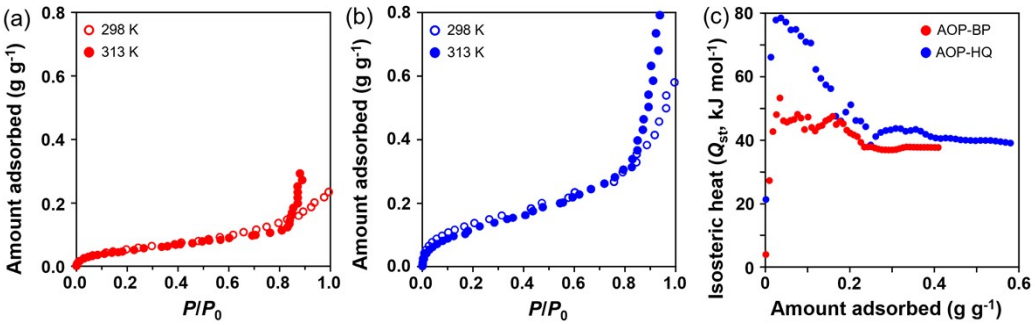

Fig. S6 H_2O adsorption isotherms of (a) AOP-BP and (b) AOP-HQ measured at 25 °C and 40 °C with (c) corresponding isosteric heat of adsorption (Q_{st}).

*The sudden increase in the H_2O adsorption at 40 °C in the high-humidity region arises from the temperature-induced decrease in the surface tension of H_2O cluster[1] and increase in the saturated vapor pressure,[2] which shifts the onset of capillary condensation to lower relative pressures.

Table S1. Assignments of FT-IR spectra in Figure 1a.

Materials	Assignments of vibrations	Wavenumber (nm^{-1})
AOP-BP	C-H stretching	2931, 2869
	C-H bending	1476
	C-H stretching (aromatic ring)	1134
	C≃C stretching (aromatic ring)	1603, 1372
	P=O stretching	1097, 1017
	O-H stretching	2972
	O-H bending	1654
	Al-O-P symmetric stretching	714, 532
	Al-O-P asymmetric stretching	966, 794
AOP-HQ	C-H stretching	2980, 2833
	C-H bending	1453
	C-H stretching (aromatic ring)	1164
	C≃C stretching (aromatic ring)	1406
	P=O stretching	1118, 1036
	O-H stretching	3058
	O-H bending	1643
	Al-O-P symmetric stretching	613, 462
	Al-O-P asymmetric stretching	956, 775

Table S2. Comparison of performance in proton conduction with benchmark materials such as Nafion or reported typical state-of-the-art inorganic and inorganic-organic hybrid proton-conducting material.

Name	Proton conductivity ($S\ cm^{-1}$)	Conditions	E_a (eV)	References
AOP-BP	2.07×10^{-3}	95% RH 90 °C	-	This work
AOP-HQ	1.31×10^{-2}		0.39	
pure AlPO	6.20×10^{-3}	95% RH 60 °C	0.38	3
AOP-Me	5.51×10^{-3}	95% RH 90 °C	-	Our previous work
AOP-Et	5.72×10^{-3}			
AOP-Ph	2.30×10^{-3}			
Nafion117	7.8×10^{-2}	100% RH 25 °C	< 0.2	4
Nafion212	6.6×10^{-2}	100% RH 20 °C	0.19	5
JU103	3.6×10^{-3}	98% RH	0.21	6

		20 °C		
$ZrP{\cdot}0.8PrNH_2{\cdot}5H_2O$	1.2×10^{-3}	90% RH 20 °C	1.04	7
$Zr(P2O7)_{0.81}(O_3POH)_{0.38}$	1.3×10^{-3}		0.19	
$(C_2N_2H_{10})_{0.5}CoPO_4$	2.1×10^{-3}	98% RH 56 °C	1.01	8
UiO-66(Zr)-SO_3H	0.34×10^{-2}	97% RH 30 °C	0.27	9
UiO-66(Zr)-$(COOH)_2$	0.10×10^{-2}		0.18	
MOF-808(Zr)	3.14×10^{-3}	99% RH 25 °C	0.37	10
Cu-SAT	0.53×10^{-3}	98% RH 80 °C	0.23	11
Na-HPAA	5.6×10^{-3}	98% RH 24 °C	0.39	12
K-HPAA	1.3×10^{-3}		0.98	
PCMOF-5(Li)	6.0×10^{-3}	95% RH 85 °C	0.17	13
PCMOF-5(Pr)	3.9×10^{-3}		0.17	
CP-1(Ho)	4.56×10^{-3}	95% RH 80 °C	0.38	14
CP-1(Er)	6.59×10^{-3}		0.32	
[Fe(ox)·$2H_2O$]	1.3×10^{-3}	98% RH 25 °C	0.37	15
Co-MOF-74	8×10^{-6} (*a*-axis)	95% RH 90 °C	-	16
	4.5×10^{-3} (*c*-axis)		0.12	
	2.5×10^{-7} (pellet)		0.30	
$[In(IA)_2\{(CH_3)_2NH_2\}(H_2O)_2]$	3.4×10^{-3}	98% RH 27 °C	0.61	17
$\{[(Me_2NH_2)_3(SO_4)]_2[Zn_2(ox)_3]\}_n$	4.2×10^{-2}	98% RH	0.13	18
$[(Cu^{I}_4Cu^{II}_4L_4){\cdot}3H_2O]_n$	1.13×10^{-2}	98% RH 100 °C	0.37	19
MIL-101(Cr)-NH-$(CH_2)_3SO_3H$	4.8×10^{-3}	95% RH 90 °C	-	20
BUT-8(Cr)A	1.27×10^{-1}	100% RH 80°C	-	21
MIP-202(Zr)	1.1×10^{-2}	95% RH 90°C	0.22	22
UiO-66-$(SO_3H)_2$	8.4×10^{-2}	90% RH 80°C	0.32	23
IM-UiO-66-AS	$> 10^{-2}$	100% RH 70°C	0.34	24
VNU-15	2.9×10^{-2}	60% RH 95°C	0.22	25
MIP-177-SO_4H-LT	2.6×10^{-2}	95% RH 25°C	-	26
$[\{(Zn_{0.25})_8(O)\}Zn_6(L)_{12}(H_2O)_{29}(DMF)_{69}(NO_3)_2]_n$	2.3×10^{-3}	95% RH 25°C	0.63	27
$MgH_6ODTMP{\cdot}6H_2O$	1.6×10^{-3}	100% RH 19°C	0.31	28
$Ti^{IV}Ti^{IV}(HPO_4)_4$	1.2×10^{-3}	95% RH 25°C	0.13	29

Table S3. Porosity data of AOP-type mesoporous materials prepared using Pluronic P123.

Materials	N_2-S_{BET} (m^2 g^{-1})	V_{total} (cm^3 g^{-1})	Pore size (nm)	Reference
AOP-BP	223	0.29	8.1	This work
AOP-HQ	316	0.42	8.1	
pure AlPO	356	0.56	8.1	3
AOP-Me	357	0.45	8.1	Our previous work
AOP-Et	378	0.76	8.1	
AOP-Ph	423	0.45	8.1	

Supplemental References

1. M. Thommes and K. A. Cychosz, *Adsorption*, 2014, **20**, 233-250.
2. M. V. Solovyeva, A. I. Shkatulov, L. G. Gordeeva, E. A. Fedorova, T. A. Krieger and Y. I. Aristov, *Langmuir*, 2021, **37**, 693-702.
3. T. Ami, K. Oka, H. Kasai and T. Kimura, *J. Mater. Chem. A*, 2026, **14**, 3863-3873.
4. Y. Sone, P. Ekdunge and D. Simonsson, *J. Electrochem. Soc.*, 1996, **143**, 1254.
5. T. Saito, Y. Matsuo, K. Tabata, T. Makino, T. Nohara and A. Masuhara, *Energy Fuels*, 2024, **38**, 4645-4652.
6. Y. Sun, Y. Yan, Y. Wang, Y. Li, J. Li and J. Yu, *Chem. Commun.*, 2015, **51**, 9317-9319.
7. M. Casciola, U. Constantino and S. D'Amico, *Solid State Ionics*, 1986, **22**, 127-133.
8. M. Wang, H. B. Luo, S. X. Liu, Y. Zou, Z. F. Tian, L. Li, J. L. Liu and X. M. Ren, *Dalton Trans.*, 2016, **45**, 19466-19472.
9. F. Yang, H. Huang, X. Wang, F. Li, Y. Gong, C. Zhong and J. R. Li, *Cryst. Growth Design*, 2015, **15**, 5827-5833.
10. H. B. Luo, M. Wang, S. X. Liu, C. Xue, Z. F. Tian, Y. Zou and X. M. Ren, *Inorg. Chem.*, 2017, **56**, 4169-4175.
11. R. Moi, A. Ghorai, S. Banerjee and K. Biradha, *Cryst. Growth Design*, 2020, **20**, 5557-5563.
12. M. Bazaga-García, M. Papadaki, R. M. P. Colodrero, P. Olivera-Pastor, E. R. Losilla, B. Nieto-Ortega, M. Á. G. Aranda, D. Choquesillo-Lazarte, A. Cabeza and K. D. Demadis, *Chem. Mater.*, 2015, **27**, 424-435.
13. N. E. Wong, P. Ramaswamy, A. S. Lee, B. S. Gelfand, K. J. Bladek, J. M. Taylor, D. M. Spasyuk and G. K. H. Shimizu, *J. Am. Chem. Soc.*, 2017, **139**, 14676-14683.
14. S. P. Bera, A. Mondal, S. Roy, B. Dey, A. Santra and S. Konar, *Dalton Trans.*, 2018, **47**, 15405-15415.

15. T. Yamada, M. Sadakiyo and H. Kitagawa, *J. Am. Chem. Soc.*, 2009, **131**, 3144-3145.
16. S. Hwang, E. J. Lee, D. Song and N. C. Jeong, *ACS Appl. Mater. Interfaces*, 2018, **10**, 35354-35360.
17. T. Panda, T. Kundu and R. Banerjee, *Chem. Commun.*, 2013, **49**, 6197-6199.
18. S. S. Nagarkar, S. M. Unni, A. Sharma, S. Kurungot and S. K. Ghosh, *Angew. Chem. Int. Ed.*, 2014, **53**, 2638-2642.
19. R. Liu, L. Zhao, S. Yu, X. Liang, Z. Li and G. Li, *Inorg. Chem.*, 2018, **57**, 11560-11568.
20. S. Devautour-Vinot, E. S. Sanil, A. Geneste, V. Ortiz, P. G. Yot, J. S. Chang and G. Maurin, *Chem. Asian J.* , 2019, **14**, 3561-3565.
21. S. Wang, M. Wahiduzzaman, L. Davis, A. Tissot, W. Shepard, J. Marrot, C. Martineau-Corcos, D. Hamdane, G. Maurin, S. Devautour-Vinot and C. Serre, *Nat. Commun.*, 2018, **9**, 4937.
22. F. Yang, G. Xu, Y. Dou, B. Wang, H. Zhang, H. Wu, W. Zhou, J. R. Li and B. Chen, *Nature Energy*, 2017, **2**, 877-883.
23. W. J. Phang, H. Jo, W. R. Lee, J. H. Song, K. Yoo, B. Kim and C. S. Hong, *Angew. Chem. Int. Ed.*, 2015, **54**, 5142-5146.
24. Y. B. Lu, Y. Q. Liao, L. Dong, S. D. Zhu, H. R. Wen, J. Huang, X. X. Dai, P. Lian, X. M. Jiang, R. Li and Y. R. Xie, *Chem. Mater.*, 2021, **33**, 7858-7868.
25. T. N. Tu, N. Q. Phan, T. T. Vu, H. L. Nguyen, K. E. Cordova and H. Furukawa, *J. Mater. Chem. A*, 2016, **4**, 3638-3641.
26. M. Wahiduzzaman, S. Wang, J. Schnee, A. Vimont, V. Ortiz, P. G. Yot, R. Retoux, M. Daturi, J. S. Lee, J. S. Chang, C. Serre, G. Maurin and S. Devautour-Vinot, *ACS Sustain. Chem. Eng.*, 2019, **7**, 5776-5783.
27. S. Sen, N. N. Nair, T. Yamada, H. Kitagawa and P. K. Bharadwaj, *J. Am. Chem. Soc.*, 2012, **134**, 19432-19437.
28. R. M. P. Colodrero, P. Olivera-Pastor, E. R. Losilla, D. Hernández-Alonso, M. A. G. Aranda, L. Leon-Reina, J. Rius, K. D. Demadis, B. Moreau, D. Villemin, M. Palomino, F. Rey and A. Cabeza, *Inorg. Chem.*, 2012, **51**, 7689-7698.
29. P. G. M. Mileo, T. Kundu, R. Semino, V. Benoit, N. Steunou, P. L. Llewellyn, C. Serre, G. Maurin and S. Devautour-Vinot, *Chem. Mater.*, 2017, **29**, 7263-7271.